

DOC RESEARCH AND DEVELOPMENT SERIES 359

Assessing the use of UAV-collected data for characterising the distributions and frequencies of sand dune vegetation cover types at Kaitorete Spit, Canterbury

Bradley S. Case, Hannah L. Buckley, Michael Fake, Stacey Bryan, Joshua Bilkey and James Griffiths



Department of
Conservation
Te Papa Atawhai

DOC Research & Development Series is a published record of scientific research carried out, or advice given, by Department of Conservation staff or external contractors funded by DOC. It comprises reports and short communications that are peer-reviewed.

This report is available from the departmental website in pdf form. Titles are listed in our catalogue on the website, refer www.doc.govt.nz under *Publications*, then *Series*.

© Copyright July 2019, New Zealand Department of Conservation

ISSN 1177-9306 (web PDF)

ISBN 978-1-98-851496-3 (web PDF)

This report was prepared for publication by the Publishing Team; editing and layout by Lynette Clelland. Publication was approved by The Director, Threats Unit, Department of Conservation, Wellington, New Zealand.

Published by Publishing Team, Department of Conservation, PO Box 10420, The Terrace, Wellington 6143, New Zealand.

In the interest of forest conservation, we support paperless electronic publishing.

CONTENTS

Abstract	1
1. Introduction	2
2. Objectives	4
3. Methods	5
3.1 Study site	5
3.2 UAV image data collection	6
3.3 Image data pre-processing	6
3.4 Field data collection	8
3.5 UAV image classification and accuracy assessment	8
3.6 Comparison of field-sampled and image-classified data	9
4. Results	11
4.1 Vegetation cover types discernible within the imagery	11
4.2 Image classification of vegetation cover types and accuracy assessments	12
4.3 Field data and image classification comparisons	13
5. Discussion	16
5.1 Image classification and cover type discrimination	16
5.2 Correspondence of image- and field-sampled data	18
6. Conclusions and recommendations	19
7. Acknowledgements	21
8. References	21
9. Glossary of terms	24

Assessing the use of UAV-collected data for characterising the distributions and frequencies of sand dune vegetation cover types at Kaitorete Spit, Canterbury

Bradley S. Case¹, Hannah L. Buckley¹, Michael Fake², Stacey Bryan², Joshua Bilkey¹ and James Griffiths³

¹ School of Science, Auckland University of Technology, Auckland, New Zealand
Bradley.Case@aut.ac.nz

² Department of Ecology, Faculty of Agriculture and Life Sciences, Lincoln University, Canterbury, New Zealand

³ Department of Conservation, PO Box 10-420, Wellington, New Zealand

Abstract

Unmanned aerial vehicles (UAVs or ‘drones’) may provide cost- and time-effective approaches for gathering information for use in ecosystem assessment and monitoring. In this scoping study focussed on the sand dune system at Kaitorete Spit, Canterbury, we assessed the ability to discriminate plant and non-plant cover type information in UAV-collected multispectral imagery, in comparison with cover types derived from field data collected using plant plot surveys. Results showed that supervised image classification generated accurate and reliable cover type information for most cover types across the study area relative to those identified from the plot surveys. A number of important species, such as pīngao (*Ficinia spiralis*), muehlenbeckia (pōhuehue, *Muehlenbeckia complexa*) and tree lupin (*Lupinus arboreus*) could be differentiated in the imagery; for other cover types, there was inadequate spectral differentiation among individual species, resulting in discrimination only among mixed vegetation complexes. Overall accuracies of discrimination were in the range of 85 to 95%. Further, at 59 field plot locations, the relative proportions of most dominant cover types derived from image classifications correlated well with those quantified from field surveys. These initial results lend confidence in the use of UAVs to effectively and rapidly collect spatially-explicit data on cover type distributions, as a complement to ground-based surveys and/or to provide regular ecosystem updates at broader scale than survey work allows. We recommend that further work be carried out to quantify the standards with which UAV aerial surveys can be used most effectively for ecological monitoring purposes and the ultimate cost-benefit tradeoffs.

Keywords: drones, multispectral data, sand dunes, biodiversity, image classification, coastal, New Zealand, pīngao, remote sensing

© Copyright July 2019, Department of Conservation. This paper may be cited as:

Case, B.S.; Buckley, H.L.; Fake, M.; Bryan, S.; Bilkey, J.; Griffiths, J. 2019: Assessing the use of UAV-collected data for characterising the distributions and frequencies of sand dune vegetation cover types at Kaitorete Spit, Canterbury. DOC Research and Development Series 359. Department of Conservation, Wellington. 25 p.

1. Introduction

New Zealand is facing unprecedented rates of biodiversity decline (Walker et al. 2006; WWF 2012). Government strategies and initiatives, including the New Zealand Biodiversity Strategy (DOC & MfE 2000) and the National Science Challenges – New Zealand Biological Heritage theme (<http://www.biologicalheritage.nz/>), recognise the need for increased and improved assessment, monitoring and reporting of New Zealand’s ecosystems in terms of their properties, functions and the biodiversity values that they support. To make informed decisions regarding the management of biodiversity, conservation and resource managers require robust information on the distribution of taxa across diverse environments and the rate at which their distributions and abundances are changing through time.

To support the assessment and monitoring of threatened ecosystems, there is currently a range of publicly-available spatial datasets that provide vital characterisations of vegetation and landcover types (e.g. Landcover database v.4.1 – <http://www.lcdb.scinfo.org.nz>), terrestrial and freshwater environments (Land Environments of New Zealand (LENZ) – Leathwick et al. 2002), Freshwater Ecosystems of New Zealand (FENZ) – Leathwick et al. 2007), soil types and properties (S-map – <https://smap.landcareresearch.co.nz>), climate (e.g. Wratt et al. 2006), and topography (Barringer et al. 2002). These national datasets are complemented by satellite imagery purchased under ‘All-of-Government’ initiatives, such as Kiwimage Quickbird imagery (<http://www.linz.govt.nz/land/maps/linz-topographic-maps/imagery-orthophotos/kiwimage>) and Land-use and Carbon Analysis System (LUCAS) project imagery (<https://www.mfe.govt.nz/more/data/available-datasets/satellite-data-search>), as well as high-resolution aerial photography that is collected regularly by regional councils. While these datasets provide valuable information for regional-to-national-scale ecological assessment, their resolution is often too coarse, both spatially and in terms of information content, to address finer-scale biodiversity and ecosystem assessment objectives. They are snapshot datasets that typically have a 5–10-year data capture frequency. Further, availability and representation of field-collected data on the distribution and abundance of specific taxa and ecosystem properties across New Zealand’s environments is patchy, largely because field surveys are costly and typically driven by the requirements of particular research projects or funding sources, rather than the needs of ecosystem assessment per se. The result is often an inadequate spatial representation of biodiversity across New Zealand’s ecosystems.

Unmanned aerial vehicles (UAVs or ‘drones’) are small, remote-piloted, fixed-wing or multi-rotor aircrafts that can be deployed with a variety of sensors to record various types of data across relatively small to moderately-large areas, and at lower altitudes (providing higher resolution) than conventional aerial (satellite-, airplane- and helicopter-based) methods. The types of data collected with a UAV depend on the sensor(s) deployed on it, and can include traditional digital colour images, video footage, infrared (multispectral and thermal) imagery, hyperspectral imagery and Light Detection and Ranging (LiDAR) data. UAVs would therefore appear to offer many benefits for ecological data collection (Cruzan et al. 2016), allowing data to be collected at resolutions that could provide a key linkage between cost- and time-intensive field surveys and coarser-scale snapshot datasets from currently-available satellite and aerial imagery (Anderson & Gaston 2013). Higher resolutions enable the potential delineation of very small features such as individual plants (Fig. 1). UAVs have other advantages. They:

- Permit collection of imagery in cloudy weather that would normally preclude higher-flying craft.
- Allow imagery to be collected more frequently, enabling the quantification of change in features over time and at appropriate times (e.g. during plant flowering).
- Can easily deploy different sensors (as required).
- Are relatively easy and inexpensive to use.

Recent studies have illustrated how UAVs can be effective in monitoring and measuring characteristics of many types of ecosystems, such as rangeland habitat (Breckenridge et al. 2012), forest diversity (Getzin et al. 2012; Lisein et al. 2015), animal population numbers and habitat suitability (Koski et al. 2009; Koh & Wich 2012; Sardá-Palomera et al. 2012; Ratcliffe et al. 2015). Despite the clear potential of UAV technologies for ecological data collection, there remains little evidence to date of the types and content of UAV-extracted information that is of relevance for ecological assessment and monitoring across New Zealand's ecosystems. So far, their most common survey and monitoring use in New Zealand appears to be in the agriculture and horticulture industries (e.g. Farmax 2014; von Bueren et al. 2014, 2015). There has also been a large amount of recent media coverage on the potential for drone use, particularly in monitoring stock and land damage from natural phenomena such as drought or flooding (Quin 2014; Robb 2014; Taranaki Daily News 2014; Tipa 2014; Callaghan Innovation 2015; Hart 2015; MacLean 2015; Wilhelmson 2015), and UAVs are increasingly used by news agencies to report on events such as natural catastrophes. Scientific literature on UAV use for planned, scientific data collection in New Zealand is limited to just a handful of studies. Two papers report using the Kahu UAV to collect data on relative humidity and temperature (Garrett et al. 2011; Cook et al. 2013). Another study used a digital camera in conjunction with a thermal infrared camera to obtain detailed information on geothermal surface features (Nishar et al. 2016). As yet there appear to be no published UAV-related ecological studies in New Zealand.

Of particular interest, from a conservation assessment and monitoring perspective, is whether there is the potential for cost savings by using UAV data collection either in place of, or supplementary to, field surveys. Currently, the potential for UAV survey data to provide very-high-resolution information (e.g. Fig. 1) on vegetation composition and distribution

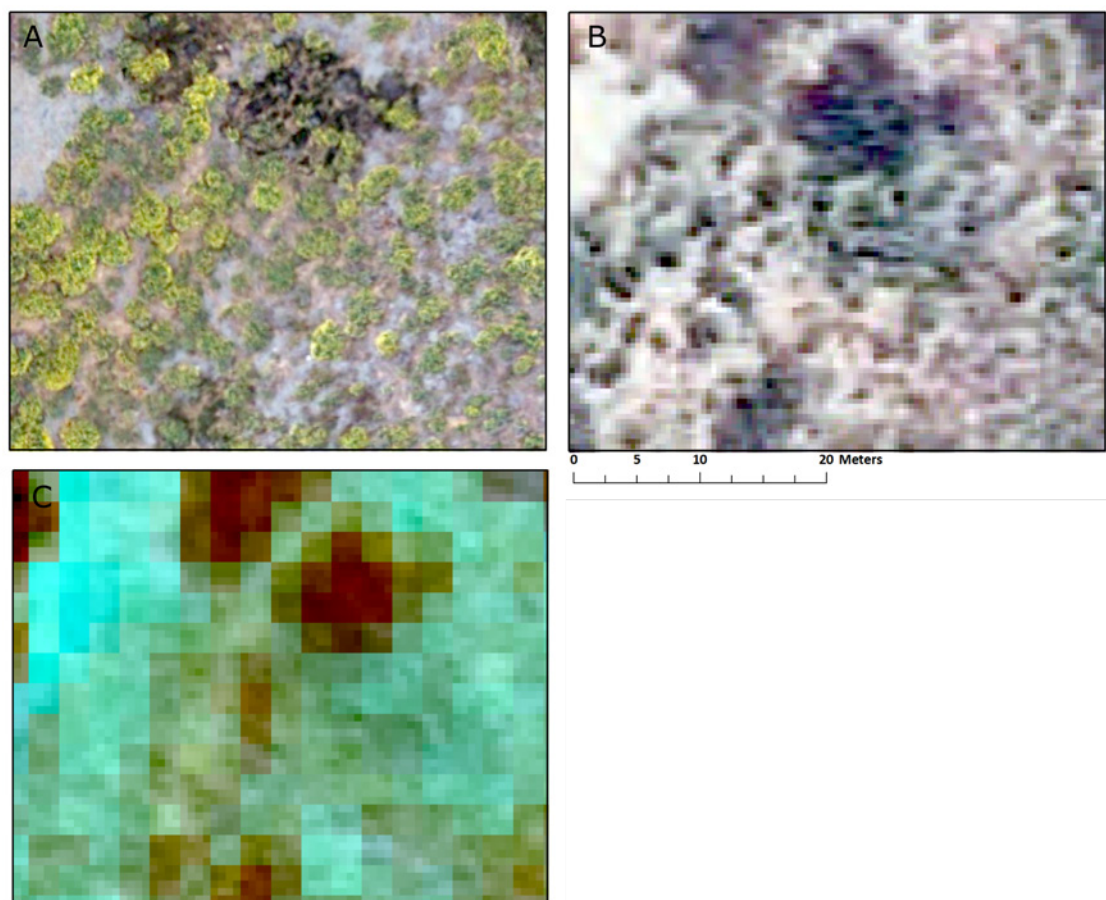


Figure 1. An illustration of differences in discernible sand dune cover types at one location for three types of image data: A. UAV-collected RGB data at a 10-cm resolution. B. Aerial RGB imagery at a 40-cm resolution. C. Quickbird satellite false-colour image from the Kiwimagery repository at 2.4-m resolution. In A, yellowish plants are flowering *Lupinus arboreus* (tree lupin), darker vegetation (dark red in C) is *Muehlenbeckia complexa*, and lighter areas are low grasses and bare ground.

(particularly for the monitoring of invasive and threatened species), the effects of weed spray operations on non-target species, and the characterisation of species' habitats has yet to be fully investigated. For example, one common use of remotely-obtained imagery is as a basis for 'image classification', whereby putative vegetation or land cover types are identified and classified using a semi-automated, computer-based procedure (Jensen 2005). In this procedure, a computer is used to discriminate among the vegetation and non-vegetation cover types identified by an analyst within the imagery and to ultimately classify all pixels across the full image. For UAV-collected imagery, this procedure is made more complex by the extremely high spatial resolutions afforded by UAV data and, therefore, the sheer volume of data requiring processing (Laliberte et al. 2011). Thus, studies are urgently needed to demonstrate the usefulness of UAV-collected imagery for image classification purposes.

This present study aims to describe procedures undertaken to generate a vegetation cover classification of UAV imagery collected over the dune ecosystem at Kaitorete Spit, Canterbury. Dune systems are an ideal test-case for the assessing the suitability of information derived from UAV-collected imagery technology as they are typically of simple topography with clear zonation of vegetation and provide easy-access for vegetation field surveys that can be used as data for validating image classification results. While sand dune habitats are relatively common in New Zealand, most have been considerably modified (Pegman & Rapson 2005) and have been decreasing in area over recent decades, with a reduction in dune area of about 70% from predicted pre-human extent (Hilton et al. 2000). Causes of this include: land development for housing; plantation forestry; stock grazing; sand mining; waste disposal; the introduction of exotic flora such as marram grass (*Ammophila arenaria*) and tree lupins (*Lupinus arboreus*) to stabilise active dunes for afforestation; and property protection (Hilton et al. 2000; Hilton 2006; Verhoeven et al. 2014). Such dramatic loss of habitat has resulted in displacement of native species (Oliphant 2014) and left sand-dune-restricted species, such as the endemic katipo spider (*Latrodectus katipo*) (Patrick 2002; Griffiths et al. 2005) and pīngao (sand sedge, *Ficinia spiralis*) (Hilton et al. 2005), threatened or in decline. In this study, we provide results from a case study aimed at assessing the application of UAV-collected data to describe spatial variation in sand dune vegetation at Kaitorete Spit, Canterbury.

2. Objectives

1. To determine the level of specificity and accuracy to which dominant species and cover types can be discriminated in UAV-collected multispectral imagery across sand dune systems at Kaitorete Spit. In this context, we were particularly interested in exploring whether key native and exotic species could be accurately identified using supervised image classification.
2. To assess how image classification data compare with field-collected data. Specifically, we sought to determine to what degree the relative abundances of dominant vegetation cover types, and overall community patterns, could be reliably represented using UAV-collected imagery.

3. Methods

3.1 Study site

Kaitorete Spit (Fig. 2) is a narrow, 28-km long (4855 ha) barrier beach located south of Banks Peninsula, Canterbury, separating Lake Ellesmere/Te Waihora from the Pacific Ocean (Fig. 2). The Spit formed as the result of long-shore drift and deposition of river gravels derived mainly from the nearby Rakaia River (Armon 1970). Across its width, Kaitorete Spit comprises three main zones (Department of Lands and Survey 1985):

- An inland zone of shingle terraces and old dune remnants
- A middle coastal dune complex
- A steep shingle beach

The middle sand dune complex, characterised by alternating dune ridges and deflation hollows (or 'blowouts'), comprises mainly coarse, grey, Kairaki sand which promotes dune stabilisation (Peace 1975). Further, relative to other dune systems in New Zealand, Kaitorete Spit is unique in having a gravelly basement layer that restricts the occurrence of dune deflation to above the water table, thereby preventing the formation of moist, inter-dune slacks (Peace 1975). The imagery collected for this study (see 3.2 below) encompasses a large portion of the full Kaitorete Spit dune complex, including the smaller Kaitorete Spit Scientific Reserve which is managed by the Department of Conservation (DOC).

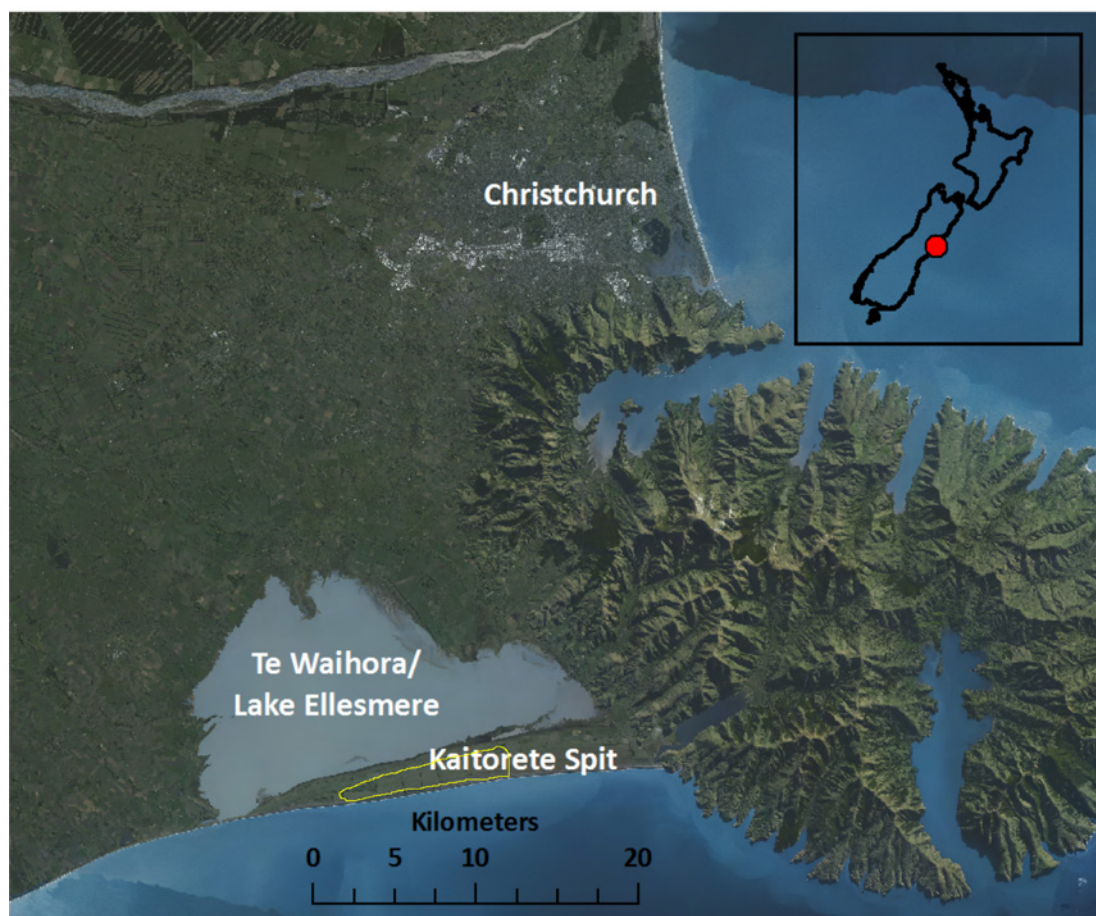


Figure 2. Location of Kaitorete Spit. Background image derived from SPOTMaps New Zealand dataset, available from the Ministry for the Environment under NZ Government and Commercial License. The area covered by the UAV flights is outlined in yellow.

The vegetation of the beach complex has been described in detail previously (Peace 1975; Widodo 1997), but generally progresses from the beach inland as follows:

- (i) A high density of pīngao on foredunes facing the beach.
- (ii) A mixture of native species such as muehlenbeckia, (*Muehlenbeckia complexa*) shore bindweed (*Calystegia soldanella*) and several *Coprosma* species along with invasive exotic weeds such as tree lupin, haretail (*Lagurus ovatus*) and catsear (*Hypochoeris radicata*). Associations of raoulia (common mat daisy, *Raoulia australis*) with a variety of native and exotic herbaceous, sedge and lichen species in deflation hollows.
- (iii) Associations among a range of native species, including muehlenbeckia, the at-risk endemic prostrate broom (*Carmichaelia appressa*), bracken fern (*Pteridium esculentum*), silver tussock (*Poa cita*) and exotics such as ripgut brome grass (*Bromus diandrus*), haretail, sorrel (*Rumex acetosella*) and catsear on the old dunes and sand flats occurring further inland. Some of these inland remnant dunes are grazed by cattle.

3.2 UAV image data collection

Image data were collected on December 5, 2013 by Hawkeye UAV Ltd. using a fixed-wing, AeroHawk RQ-84Z UAV aircraft, flown at an average height of 190 m above sea level. The UAV was fitted with dual-mounted, Sony NEX-5 high-resolution cameras in the Sony ARW format, which were used to collect spectral data for individual red, green, blue (RGB) visible wavelength bands and a near infrared (NIR) wavelength band. These multispectral image data were collected as snapshots taken at fixed time intervals, calibrated to the altitude and velocity of the aircraft to ensure that there was at least 60% overlap among adjacent snapshots, enabling accurate photogrammetric calibration and orthorectification of the image data (see next section and Glossary).

3.3 Image data pre-processing

To prepare collected UAV snapshot images for subsequent supervised image classification processing, a series of data ‘pre-processing’ steps were carried out using specialised computer software. These steps consisted of:

1. **Photogrammetric calibration and orthorectification** – the removal of variation in the collected spectral data caused by movement in the aircraft during collection and by terrain variability.
2. **Mosaicing and colour-balancing** – production of a single image ‘mosaic’ from the multiple snapshots collected by the UAV sensor(s), for each band of spectral data (e.g. R, G, B and NIR bands), and the balancing of variations in the spectral qualities (i.e. colour or brightness values) across all image snapshots.
3. **Geo-referencing** of image dataset – the spatially-positioning in geographic coordinate space of the mosaiced image so it could be used accurately within a Geographic Information System (GIS).

For this study, thirty 1 × 1 m **calibration targets**, visible within the collected imagery, were laid out across the area prior to the UAV flights, to enable the photogrammetric adjustment of the imagery. Photogrammetric calibration and image orthorectification were carried out by Hawkeye UAV Ltd. using the Aero photogrammetry software (v. 2.93), producing RGB and NIR image datasets corrected for topographic variation with a nominal resolution of 10 cm. Snapshot data were geo-referenced using the previously-mentioned ground control points and GPS data acquired during the AeroHawk’s flight using an on-board positioning system.

Snapshot images were then mosaiced and colour balanced using tools within the GIS software ArcGIS 10.3 (ESRI 2014). Through this process, considerable spectral variability was discovered among some of the snapshots that could not be adequately balanced, resulting in substantial

variation across the mosaiced imagery. The largest source of variation was from the image data being collected in two separate sorties (on the same day). In particular, the images of the second half of the site, taken in the afternoon, displayed much more spectral distortion (i.e. extreme variation in RGB and NIR values) than the first set of images, particularly in the near-infrared band. The cause of this difference is unknown but may be due to changing atmospheric conditions at the time. Imagery collected during the first flight were spectrally balanced but displayed the greatest spatial inaccuracies, particularly for the second half of the site, which was flown without sufficient ground control targets, resulting in a decreased ability of the processing software to position the images accurately relative to true ground-based coordinates.

Geo-referencing was carried out within ArcGIS 10.3 in two stages. Due to slight discrepancies in spatial positioning between the NIR and RGB mosaiced images, these were referenced against each other as a first step. Second, the two sets of mosaiced images were then georeferenced against known ground locations that were visible in both the mosaiced images and other spatially-referenced GIS datasets, including roads, fence lines and other aerial imagery. When selecting reference points to use for this process, static features such as fence posts, corners of buildings, vertices in track unions and other objects were given priority over living features (i.e. plants) as they have more defined borders which allow for higher confidence in discernibility across both RGB and NIR images. When no suitable physical objects were available, plants with highly contrasting features or boundaries were selected as reference points. If the chosen plant was large (covering more than 20–30 pixels), then the most discernible plant feature would be used. If the plant was small (less than or 20 pixels), then the centre of the plant was used. Georeferencing was based on 275 ground reference points selected across the mosaiced images, resulting in georeferenced RGB and NIR images comprising a c. 500-ha area of Kaitorete Spit (e.g. Figs 3A, B) that were spatially-accurate to within ± 0.244 m (on average). From these two images, a normalised difference vegetation index (NDVI) raster (Fig. 3C) was computed as the difference between pixel-level NIR and Red spectral band values divided by the sum of pixel-level spectral data for these two bands; NDVI is commonly-used for discriminating among features that differ in their level of green biomass (Petorelli et al. 2005). A five-band image stack was created that contained RGB and NIR data bands, as well as a band containing the NDVI data; this image stack was subsequently used for **supervised image classification**.

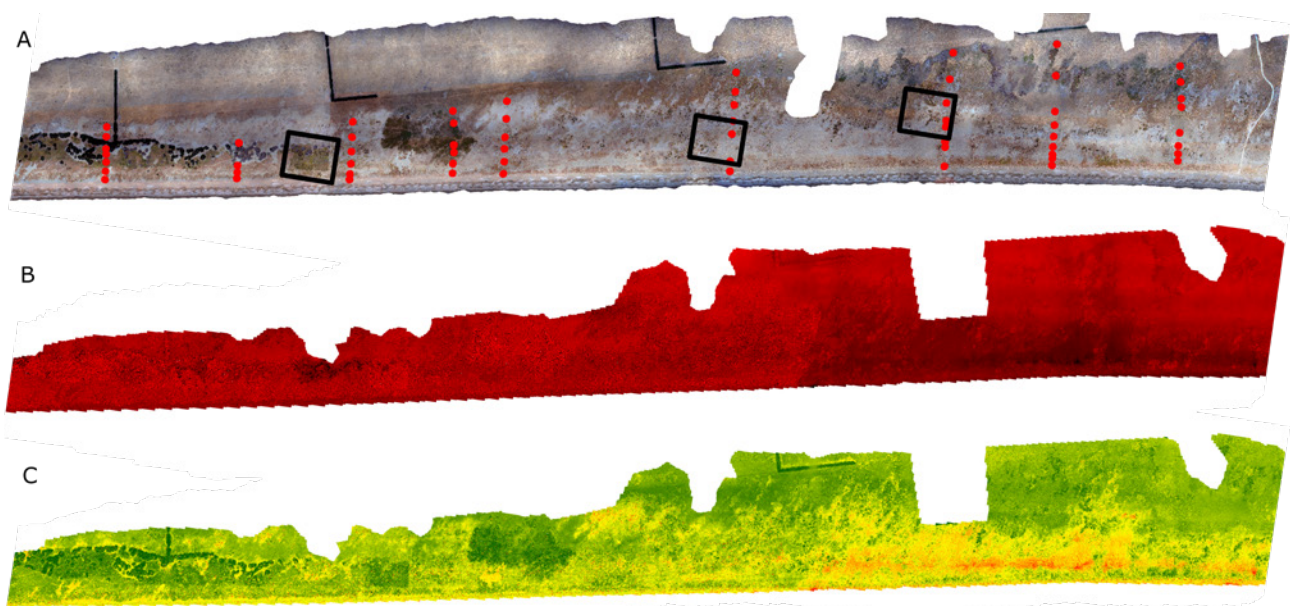


Figure 3. UAV-collected Kaitorete Spit data comprising the five-band image stack used for image classification analyses: (A) composite red, green, blue (RGB) data bands; (B) a near-infrared (NIR) data band; and (C) a normalised difference vegetation index (NDVI) data band. For the NDVI band, green colours indicate areas of moderate-to-high green biomass, yellow colours indicate areas of low green biomass, and red/orange colours indicate zones of no biomass (e.g. sand, bare ground). The black rectangles in (A) delimit the three focal areas used to assess image classification accuracy; the red dots depict the locations of field data collection plots along nine transects from beech to back dune zone.

3.4 Field data collection

In summer 2013, vegetation sampling was carried out within 64, 6 × 6 m, non-permanent plots across Kaitorete Spit, distributed along a total of nine transects (Fig. 3A). Transects were established perpendicular to the beach at random points along the length of the Spit within the known image boundary, traversing the width of the sand dune system from the high tide mark across the ridge/hollow sand dune zone, and inland to the gravel/shingle zone. Along each transect, plots were established with random inter-plot distances of 50–100 m, with the first sampling point randomly located within 1–10 m inland from the high tide mark in the foredune zone and the final plot located further inland, typically in the inland gravel/shingle zone. This resulted in six to eight plots being established along each transect. Each plot was subdivided into nine 2 × 2 m subplots. A Trimble ProXT differential GPS unit, with a horizontal accuracy of ± 1 m, was used to record the location of the centre of each subplot in New Zealand Map Grid (NZ 1949) coordinates.

Within each subplot, the relative cover proportions (%) were recorded for vegetated and non-vegetated cover types (hereafter ‘cover type frequencies’) including lichens, bryophytes, standing dead biomass, bare ground, coarse woody debris (driftwood, detritus), all grasses, all forbs, and the dominant plant species pīngao, bracken fern, prostrate broom, lupin and raoulia. The maximum height of the tallest vegetation present and the average height of most of the vegetation in each quadrat were also recorded, along with subplot maximum and average vegetation height.

3.5 UAV image classification and accuracy assessment

We carried out a supervised image classification of the UAV-collected imagery. Supervised image classification essentially involves the automatic (computer-algorithm-based) clustering or grouping of pixels in an image into relatively homogeneous classes or ‘cover types’ with multivariate statistical analyses. First, spectral data (e.g. R, G, B, NIR) from the mosaiced image are extracted for a small set of ‘training pixels’ located on the image that have a known cover type value. Second, these training data are used to generate a classification algorithm that aims to maximise the statistical separation in spectral values among the pixels for the different cover types. Third, the classification algorithm is applied to all pixels to produce a classification of the full image into cover types. Finally, the classified image is compared with a set of independently-collected ‘validation pixels’ to generate a classification accuracy table (also called a ‘confusion matrix’) that is used to evaluate the adequacy of the classification procedure. In many cases, several iterations of the above process are required to provide a useful image classification output (Jensen 2005).

The training and validation pixels can be selected visually on the image by an expert analyst who has familiarity with both the vegetation cover types on the ground and how these appear in the image, or alternatively by identifying cover types in the field and accurately locating them in the imagery using GPS coordinates. The level of specificity of the cover types (e.g. individual species v. mixtures of species) provided to the classification algorithm in the training data usually reflects how well the species and cover types seen in the field can be realistically discriminated on the image. Thus, the typical first step in the classification process is to use expert knowledge to develop a cover typology that is predicted to have a good level of success at being discriminated in the image, while also reflecting on-the-ground reality as best as possible (Jensen 2005).

For our classification procedure, the five-band image data stack was used as a basis for the automatic classification of dominant plant species, species conglomerations, and other non-plant features across 3–4-ha focal areas within the larger Kaitorete Spit study area (Fig. 3A). These focal areas were chosen as representative examples of the variation in sand dune terrain and cover

types that occur across the Kaitorete Spit dune system. RGB, NIR, and NDVI data were extracted for small 10–500-pixel areas across each focal area to form image classification training datasets. These datasets were used to train a maximum likelihood feature classifier within ArcGIS 10.3 that was then applied to generate a classified feature typology of each focal area. The training polygons were located in a **stratified random sampling design** across each focal area such that, on average, approximately 50 random training areas (comprising 100–1000+ pixels) were compiled for each of the cover types occurring within the focal areas, reflecting their relative frequencies of occurrence. Training samples were selected on-screen, within the GIS, by one person who had a high degree of familiarity with the vegetation across the study area and was able to reliably identify these types within the imagery.

Classification accuracy assessments were carried out using an independent set of ten validation areas, comprising groups of adjacent pixels, digitised on the imagery for each of the identified cover classes for each of the three focal areas. Similar to training sample selection, validation areas were selected across the full extent of the focal images to encompass potential spatial variation in the classification, while ensuring that each cover type was sampled in proportion to its relative frequency. An image classification confusion matrix was compiled for each focal area, comparing the cover types of the pixels identified in the validation dataset with those from the classified images. From this matrix, an overall image classification accuracy was computed as the number of correctly classified pixels in the validation sample for each class divided by the total number of pixels in the validation sample. For each of the three focal areas, we also computed cover-type-specific accuracies and user reliabilities. The cover type accuracies were computed as the number of correctly classified validation pixels for a given cover type out of the number of validation samples for that type. The user reliabilities were computed as the percentage of correctly labelled pixels for each cover type out of the total number of classified pixels for each cover type in the sample set.

3.6 Comparison of field-sampled and image-classified data

A total of 59 of the field-surveyed plots, distributed along the nine field transects, fell within the bounds of the UAV imagery. The aim here was to compare the field-collected cover type data for each of these plots with the cover types emerging from an image classification at each of the plot locations. To do this, it was first necessary to minimise the total image area subjected to image classification, as the total Kaitorete Spit image was too large and spatially complex to enable the collection of adequate training samples to reliably classify the full image. Thus, the 5-band Kaitorete Spit image was clipped to each of the nine field transects and their associated plots, resulting in nine smaller ‘image transects’ that were each subjected to a supervised image classification. Supervised classification for each image transect followed the same procedure as for the focal area analysis (above): a set of training samples were collected for each cover type discernible within each image transect (Fig. 4A) and were used to carry out a supervised, maximum-likelihood classification of each transect (Fig. 4B). Subsequently, these raster-based image classifications were clipped to the extent of each plot along each image transect (Fig. 4C), converted to polygon features, and then exported to a spreadsheet. Using these data, the proportions of each image-classified cover type occurring at the location of each plot was computed.

We compared field-sampled and image-classified results across the 59 plot locations in two ways. First, we examined correlations in cover type frequencies per plot between field- and image-based results for eight dominant vegetation cover types across the images. This provided a univariate assessment of whether image classifications were providing reliable representations of **ground truth**. Second, we carried out a community-level analysis of all cover types found across plots for both the field-based and image-classified data. Because the data were cover type frequencies and were continuous in nature, we carried out principal components analysis separately on the two datasets, presenting the results in the form of bi-plots to visualise plant community differences among the plots. All analyses were carried out in R, version 3.3.3 (R Core Team 2017).

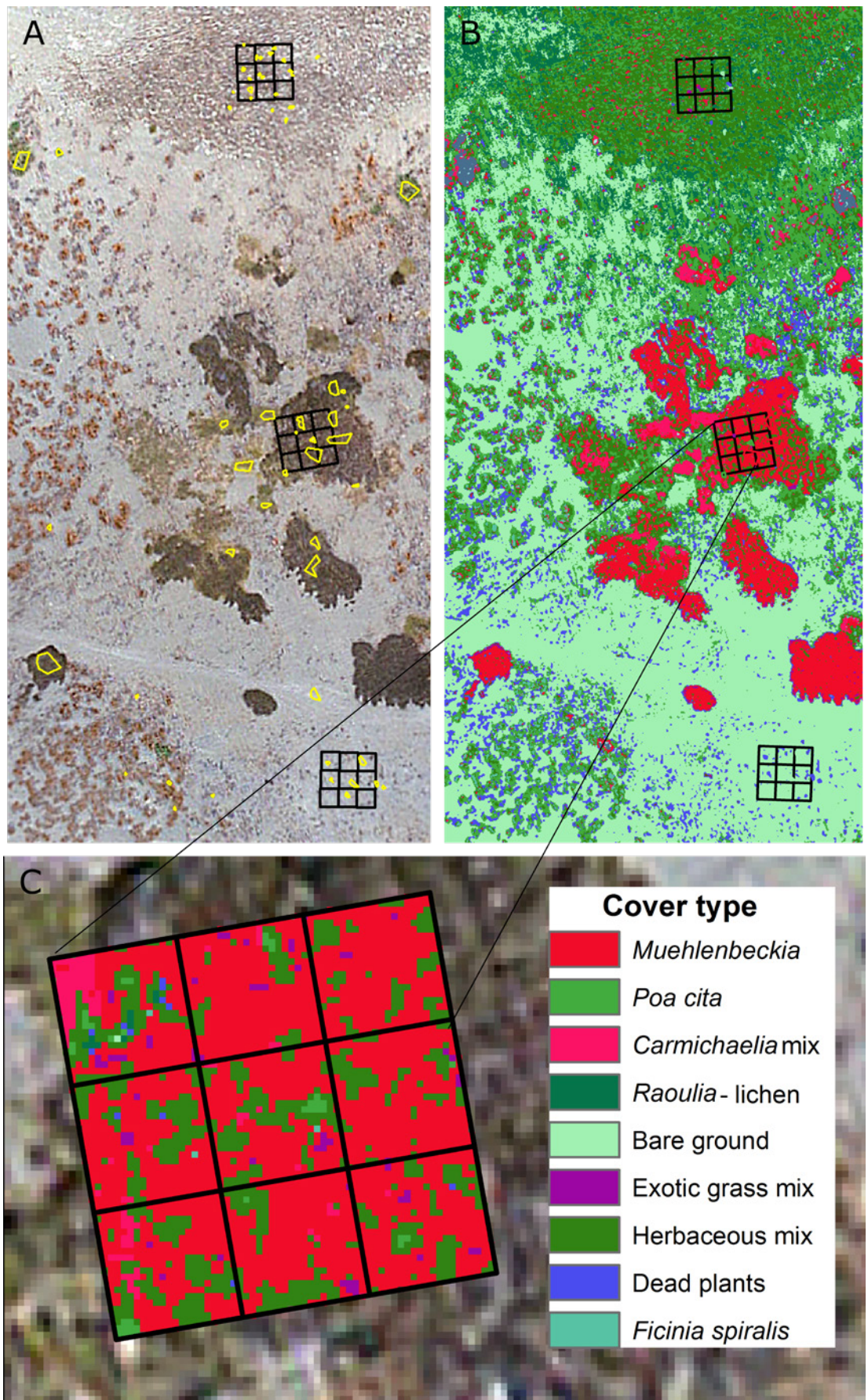


Figure 4. A portion of an 'image transect' and its associated field plots (A). Image transects are pieces of the full Kaitorete Spit UAV image clipped to the extent of each of nine field transects (see Figure 2A). The small yellow polygons in A are areas where pixel training samples for different cover types were collected to produce a supervised classification of the image transect (B). Once classified, the proportions of different cover types were extracted at each field plot location along that image transect (C), and subsequently used to compare image classification results with field-collected data.

4. Results

4.1 Vegetation cover types discernible within the imagery

A total of 16 vegetation cover types were able to be discerned within the imagery and these formed the basis for supervised image classification across the mosaiced image (Table 1). These types were determined by what was initially considered to be visible within the imagery, while generally trying to align them as much as possible to the cover types identified in the field surveys. Several of the image cover types comprised species mixtures, in that there was a dominant species or cover type intermixed with other indiscernible components (e.g. prostrate broom mix, bryophyte mix), species that were visually similar on the imagery and often occurred together (*Raoulia*-lichen), or there was a mixture of unidentifiable and largely exotic grasses (grass mix) or small herbaceous plants (herbaceous mix). The ‘grass mix’ type was typically identified in the image as taller, greener grass growing amongst the other mostly native cover types, likely due to the effects of increased nutrient availability with the proximity of these other plants. The ‘herbaceous mix’ type comprised a mix of unknown low-growing plants – likely small forbs and exotic grasses that had been grazed to ground level.

Table 1. The cover types used for supervised image classification of Kaitorete Spit UAV-collected imagery. These 16 types were established *a priori*, based on prior on-the-ground knowledge of the dune system, as well as what was deemed to be adequately discernible in the imagery upon visual inspection.

COVER TYPE DESIGNATION	DESCRIPTION
Bare ground	Mainly sand, but also exposed gravel.
<i>Ficinia spiralis</i>	Pīngao – a threatened sand-binding sedge; Kaitorete Spit has one of the largest remaining populations of this species in New Zealand.
<i>Muehlenbeckia complexa</i>	Pōhuehue – a native shrub species common to dune areas.
<i>Lupinus arboreus</i>	Tree lupin – this invasive shrub is commonly found on fore- and mid-dune areas on Kaitorete Spit and is actively managed by DOC.
<i>Raoulia australis</i> - lichen	<i>Raoulia</i> is a ground-dwelling daisy that forms mats of whitish foliage. This species often occurs in association with lichen species that are relatively indistinguishable spectrally from <i>raoulia</i> .
<i>Poa cita</i>	Silver tussock – a native tussock grass found across New Zealand.
<i>Carmichaelia appressa</i> mix	Prostrate broom – a rare species, endemic to Kaitorete Spit. While relatively distinct spectrally, it typically occurs mixed with other herbaceous plants.
<i>Pteridium esculentum</i>	Bracken fern – occurring in large, dense patches on remnant dune areas, inland on Kaitorete Spit.
Bryophyte (moss) mix	Moss species (e.g. <i>Triquetrella papillata</i>) having a distinctive spectral signature, occurring closely mixed with other small herbaceous plant species.
Herbaceous mix	A mixture of low-growing herbaceous plant species that are not discernible individually, but commonly occur in mid-dune areas between dominant cover types.
Grass mix	A mixture of fast-growing exotic grasses, typically found in close proximity to other dominant cover types, taking advantage of increased nutrients in these areas.
<i>Pinus</i> spp.	Pine trees occurring along property boundaries in inland zones of Kaitorete Spit.
Dead <i>Ficinia spiralis</i>	Dead pīngao, typically occurring as portions of live pīngao plants.
Dead <i>Pteridium esculentum</i>	Dead bracken fronds mixed within live bracken patches.
Dead plants	Other dead plants.
Driftwood	Occurring in fore dune areas.

4.2 Image classification of vegetation cover types and accuracy assessments

The three focal image areas contained 12 of the 16 cover types identified across the full image. Supervised maximum likelihood image classifications at the three focal sites (Figs 5, 6 & 7) produced overall classification accuracies of 94%, 88%, and 85% for focal areas 1, 2 and 3, respectively, across all cover types (Table 2). When assessed against validation pixels, individual cover types were classified with an accuracy greater than 80% for most types. Pines (*Pinus* spp.) and bracken fern, which were only present in focal areas 1 and 2, were not well-classified relative to field data, and ‘grass mix’ and ‘herbaceous mix’ types were not accurately classified for focal area 3. Classification reliabilities, representing the overall accuracy with which pixels were correctly labelled across the full focal images, were generally greater than 75% for most cover types; although, depending on the area, several cover types (e.g. tree lupin and bracken fern in focal area 2 and pīngao and grass mix in focal area 3) had relatively low reliabilities.

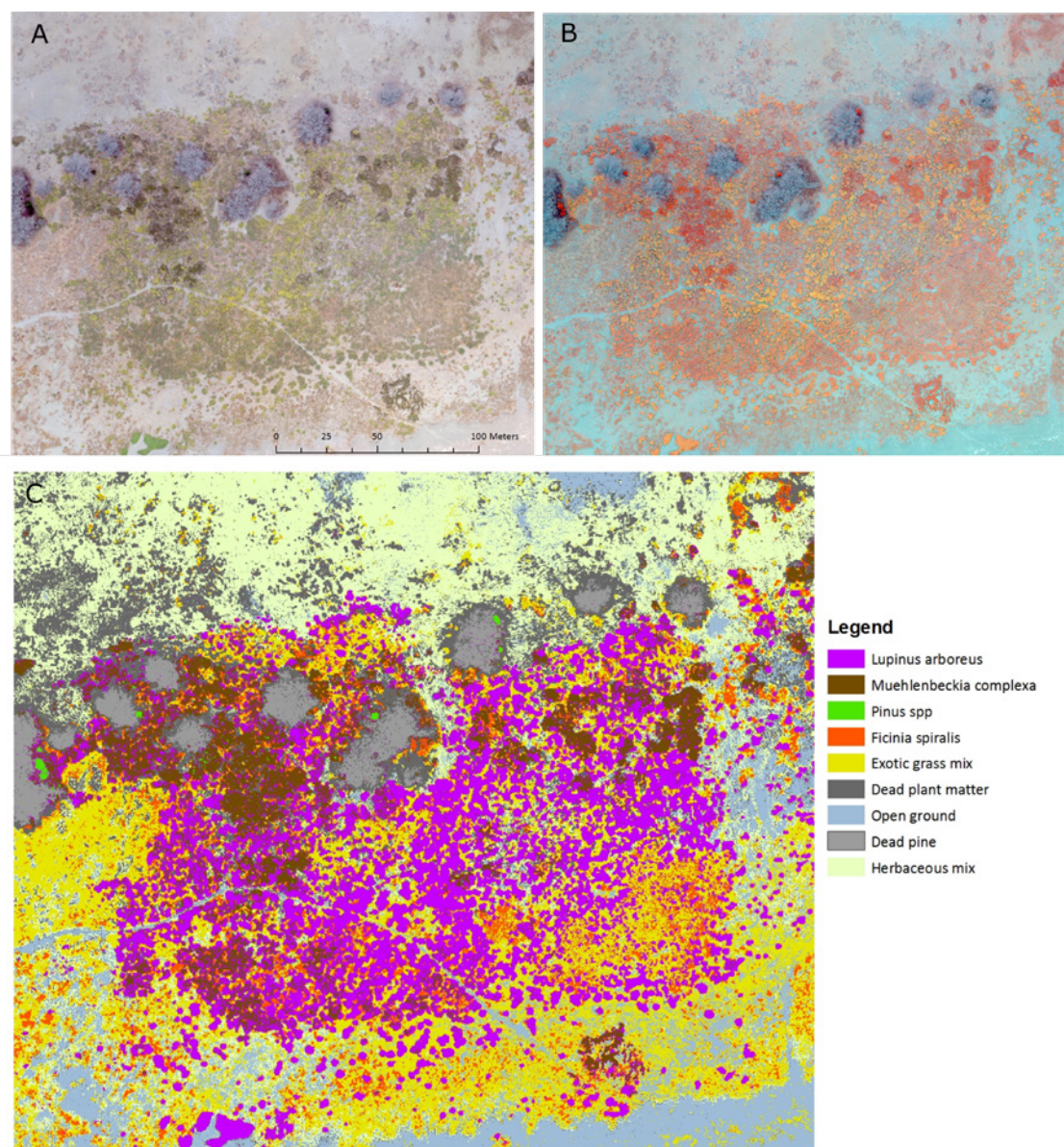


Figure 5. Focal area 1 (see Fig. 3A): (A) True colour composite image (image bands 1, 2, and 3), (B) False colour composite image (image bands 4, 2, 3), and (C) maximum likelihood image classification.

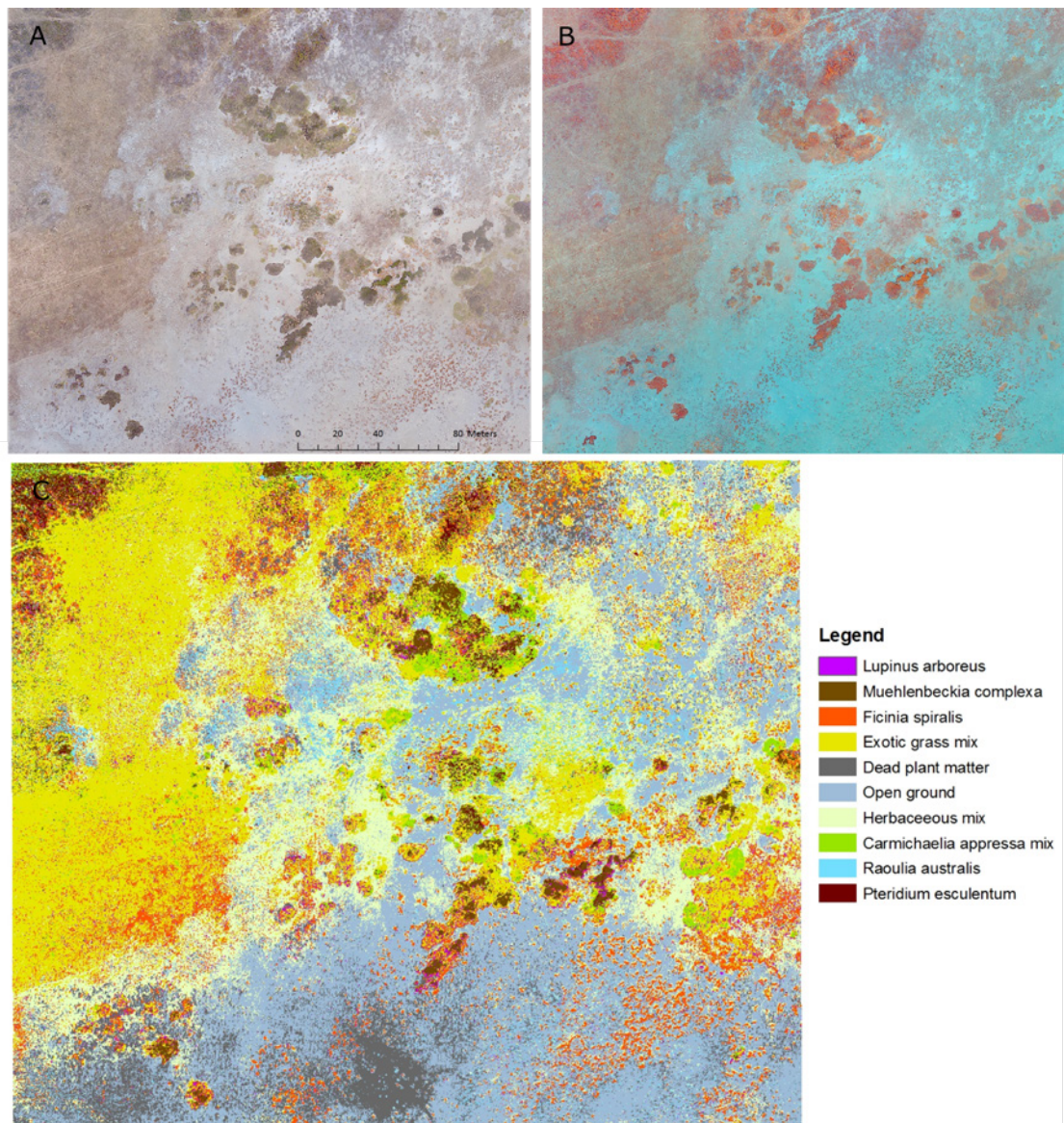


Figure 6. Focal Area 2 (see Fig. 3A): (A) True colour composite image (image bands 1, 2, and 3), (B) False colour composite image (image bands 4, 2, 3), and (C) maximum likelihood image classification.

4.3 Field data and image classification comparisons

For nine of the dominant cover types across the field plot locations (Fig. 8), correlations between field-sampled cover type proportions and those derived from image classification ranged from 0.47 to 0.84. Tree lupin and prostrate broom cover proportions were overestimated based on image classification, while *Raoulia*-lichen proportions were underestimated by image classification; there was good concordance for the other cover types.

Principal component ordinations of cover type frequencies for both the field-collected and image-classified data at plot locations showed a strong PC axis 1 gradient associated largely with the proportion of bare ground across the plots (Table 3A, B). For the field data, PC axis 1 was characterised by a weak but positive association between bare ground and the cover of pīngao, and negative associations of bare ground with all other vegetation. For image-classified data, PC axis 1 was characterised by positive but weak associations among bare ground, pīngao, and dead vegetation, and negative associations between bare ground and other vegetation types, particularly with the proportions of muehlenbeckia and herbaceous vegetation. For the field data, PC axis 2 was characterised largely by bracken fern cover proportions, which were

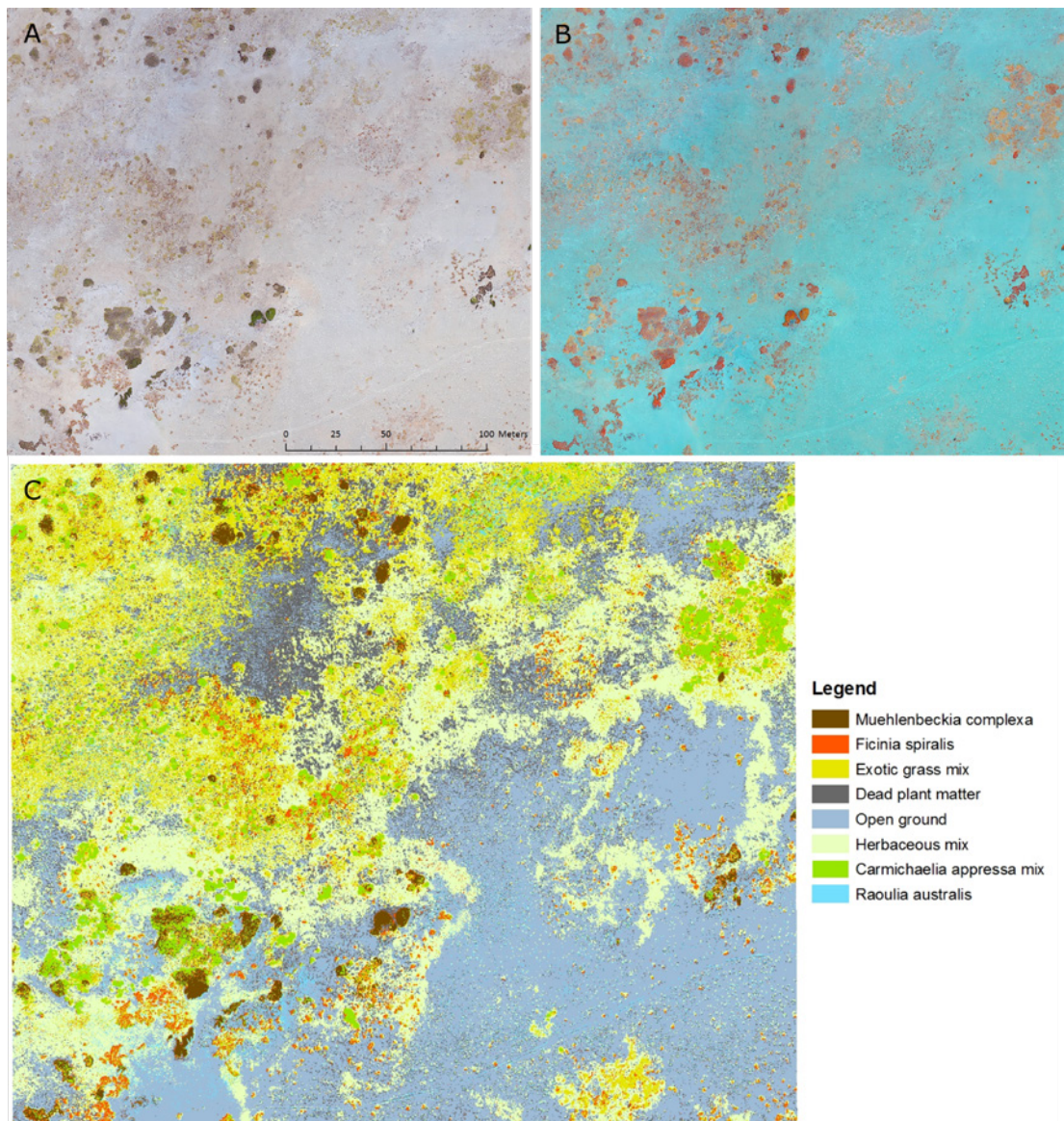


Figure 7. Focal area 3 (see Fig. 3A): (A) True colour composite image (image bands 1, 2, and 3), (B) False colour composite image (image bands 4, 2, 3), and (C) maximum likelihood image classification.

positively associated with proportions of dead bracken and other dead standing biomass, and negatively associated with the relative amount of grasses, forbs and most other vegetation types. For the image-classified data, PC axis 2 was characterised by proportions of bracken fern, muehlenbeckia, tree lupin, dead bracken and exotic grasses at one end of the gradient, which were negatively associated with the relative cover of mixed herbaceous vegetation. For the field data, PC axis 3 was characterised mainly by a negative association between muehlenbeckia cover proportions and those of bryophytes and forbs. For the image-classified data, PC axis 3 was characterised by a gradient defined by positive associations among cover proportions of pīngao, tree lupin and exotic grasses, which were negatively associated with proportions of muehlenbeckia and prostrate broom mix.

Table 2. Image classification accuracy assessment results for focal areas 1, 2 and 3 at Kaitorete Spit (see Fig. 3). For each focal area, the results show a cross-tabulation of cover types expertly-assigned to a sample of validation pixels (columns) against those assigned using a supervised, maximum-likelihood image classification (rows) trained using an independent sample of pixels. Thus, the grey diagonal boxes show the number of pixels in the validation sample correctly classified by the image classification and the values in the off-diagonals indicate the number of pixels incorrectly classified. The cover type accuracy is calculated as the percentage of validation sample pixels for each cover type correctly labelled by the image classification procedure. From the perspective of an end user of the classified image, the classification percent reliability provides some indication of how reliably any pixel in the classified image has been labelled. The overall accuracy indicates the percentage of validation sample pixels correctly classified out of the total validation sample.

FOCAL AREA 1	VALIDATION SAMPLE									Row totals	Reliability (%)
Classification	Lupin	<i>Muehlenbeckia</i>	Pine	Pīngao	Grass mix	Dead pīngao	Bare ground	Dead pine	Herbaceous mix		
Lupin	1305	37	5					1		1348	96.8
<i>Muehlenbeckia</i>	114	851	38							1003	84.8
Pine		16	71							87	81.6
Pīngao				270	1					271	99.6
Grass mix				4	447	1	19		18	489	91.4
Dead pīngao						247	15	52		314	78.7
Bare ground					80		3296			3376	97.6
Dead pine						16		416		432	96.3
Herbaceous mix					26	6	24		1028	1084	94.8
Column totals	1419	904	114	274	554	270	3354	469	1046	8404	
Cover type accuracy (%)	92.0	94.1	62.3	98.5	80.7	91.5	98.3	88.7	98.3		
Overall accuracy (%)	94.4										

FOCAL AREA 2	VALIDATION SAMPLE										Row totals	Reliability (%)	
Classification	Lupin	<i>Muehlenbeckia</i>	Pīngao	Grass mix	Dead pīngao	Bare ground	Herbaceous mix	Broom mix	<i>Raoulia</i> -lichen	Bracken			
Lupin	28	7		1						10	46	60.9	
<i>Muehlenbeckia</i>		533		2						4	21	560	95.2
Pīngao	1		176	17	6		1				201	87.6	
Grass mix	1	1	6	430			3	17			458	93.9	
Dead pīngao					63	1					64	98.4	
Bare ground	1				8	742	1		3		755	98.3	
Herbaceous mix				9		12	189				210	90.0	
Broom mix	3	4	1	9				306		3	326	93.9	
<i>Raoulia</i> lichen				6		94			101		201	50.2	
Bracken		76								19	32	127	25.2
Column totals	34	621	183	474	77	849	194	356	104	56	2948		
Cover type accuracy (%)	82.4	85.8	96.2	90.7	81.8	87.4	97.4	86.0	97.1	57.1			
Overall accuracy (%)	88.2												

FOCAL AREA 3	VALIDATION SAMPLE								Row totals	Reliability (%)
Classification	<i>Muehlenbeckia</i>	Pīngao	Grass mix	Dead pīngao	Bare ground	Herbaceous mix	Broom mix	<i>Raoulia</i> -lichen		
<i>Muehlenbeckia</i>	1239	1							1240	99.9
Pīngao	88	97	9				2		196	49.5
Grass mix	29	1	120			132	1		283	42.4
Dead pīngao	4			28	1				33	84.8
Bare ground					221				221	100.0
Herbaceous mix	6		17			123			146	84.2
Broom mix	62	3	10				277		352	78.7
<i>Raoulia</i> -lichen					2			46	48	95.8
Column totals	1428	102	156	28	224	255	280	46	2519	
Cover type accuracy (%)	86.8	95.1	76.9	100.0	98.7	48.2	98.9	100.0		
Overall accuracy (%)	85.4									

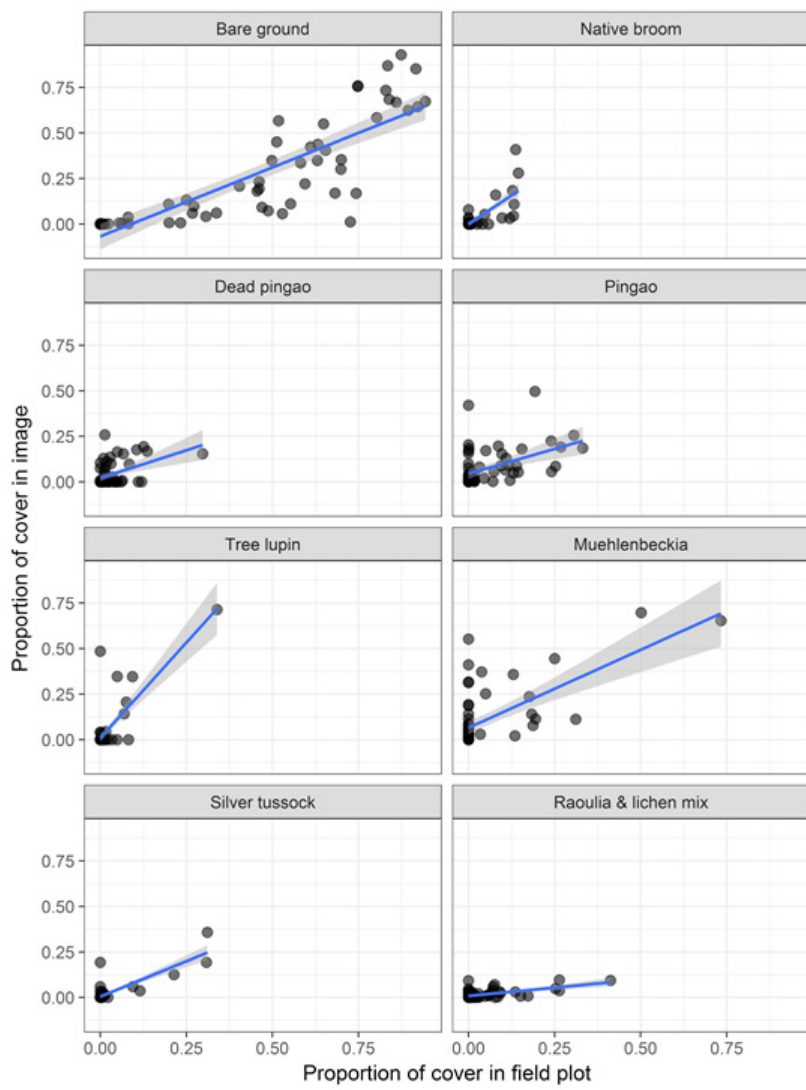


Figure 8. Correlations between image-classified and field-collected cover proportions for eight dominant cover types at 59, 2 × 2 m field plots distributed along nine transects at Kaitorete Spit.

5. Discussion

5.1 Image classification and cover type discrimination

Supervised image classification of collected UAV imagery was successful in discriminating the dominant cover types that occurred across Kaitorete Spit, relative to what was observed on the ground. Cover type classification accuracies and reliabilities ranged from 25 to 100% for the individual cover types, with the majority achieving 80% accuracy or better. Further, overall classification accuracies were in the range of 85–95%, lending confidence to the use of high-resolution UAV imagery for characterising sand dune vegetation. It was clear that the use of multispectral, as opposed to colour-only, imagery was crucial for identifying species differences as there were clear near-infrared reflectance differences among some vegetation types.

Nonetheless, the specificity with which individual species could be discriminated was variable and dependent on both the distinctiveness of a given species' spectral signature in terms of the five-band image stack dataset, and the degree to which it occurred intermixed with, or proximal to, other species and cover types across the dune system. Overall, results indicated that:

Table 3. Axis loadings for a principal components analysis of (A) field-collected cover type frequencies in 59 sample plots and (B) UAV image-classified cover type frequencies at the same plot locations. Loadings greater or equal to 0.1 are shown in bold to facilitate interpretation.

A – FIELD-SAMPLED COVER TYPES	PC1	PC2	PC3
Bare ground	0.452	-0.02	0.022
<i>Ficinia spiralis</i>	0.054	-0.002	-0.023
<i>Muehlenbeckia complexa</i>	-0.066	-0.085	-0.424
<i>Lupinus arboreus</i>	-0.008	0.003	0.004
<i>Raoulia australis</i>	-0.003	-0.035	0.073
<i>Poa cita</i>	-0.037	-0.06	0.028
<i>Carmichaelia appressa</i>	-0.023	-0.037	-0.011
<i>Pteridium esculentum</i> (bracken)	-0.057	0.37	0.017
Bryophytes	-0.078	-0.04	0.179
Lichens	-0.006	-0.025	0.001
Forbs	-0.081	-0.103	0.135
Grasses	-0.134	-0.148	0.071
dead <i>Ficinia spiralis</i>	0.024	0.015	-0.021
dead <i>Pteridium esculentum</i>	-0.039	0.174	0.02
dead SB	-0.019	0.185	-0.052
dead <i>Carmichaelia appressa</i>	0.001	-0.001	0.001
dead <i>Lupinus arboreus</i>	-0.004	-0.001	-0.058
dead <i>Lycium ferocissimum</i>	0.001	0.001	0.001
dead <i>Muehlenbeckia complexa</i>	0.001	0.001	-0.002
dead <i>Poa cita</i>	0.001	-0.001	0.001
dead <i>Raoulia australis</i>	0.001	0.001	0.001
Coarse woody debris	0.004	0.001	-0.008
<i>Lycium ferocissimum</i>	0.002	0.001	0.001
<i>Meliccytus alpinus</i>	0.001	-0.007	-0.008
<i>Pimelea prostrata</i>	0.001	0.001	0.001
<i>Ammophila arenaria</i>	0.001	0.001	0.001
Cumulative proportion of variance explained	0.567	0.666	0.751
B – IMAGE-CLASSIFIED COVER TYPES	PC1	PC2	PC3
Bare ground	-0.874	-0.204	-0.193
<i>Ficinia spiralis</i>	-0.015	0.047	0.311
<i>Muehlenbeckia complexa</i>	0.265	0.345	-0.721
<i>Lupinus arboreus</i>	0.045	0.209	0.502
<i>Raoulia australis</i> – lichen	0.001	-0.063	-0.005
<i>Poa cita</i>	0.059	-0.029	-0.053
<i>Carmichaelia appressa</i> mix	0.047	0.015	-0.114
<i>Pteridium esculentum</i> (bracken)	0.066	0.254	0.059
Bryophyte (moss) mix	0.027	-0.026	0.049
Herbaceous mix	0.371	-0.83	-0.052
Grass mix	0.075	0.111	0.25
Dead <i>Ficinia spiralis</i>	-0.072	-0.014	-0.031
Dead <i>Pteridium esculentum</i>	0.055	0.138	0.056
Dead plants	-0.041	0.051	-0.057
Driftwood	-0.009	-0.003	0.001
Cumulative proportion of variance explained	0.430	0.613	0.726

1. Pīngao, silver tussock, muehlenbeckia, tree lupin and bracken fern could be identified spectrally at the species level in the imagery. Individual plants of pīngao, silver tussock and tree lupin could be readily discerned, while muehlenbeckia was discernible as groups of plants growing together.
2. Bracken fern, although clearly evident on the imagery, was challenging to identify spectrally, largely because its spectral values overlapped with those of other cover types and also because dead or browning bracken fronds were frequently mixed amongst live fronds.
3. *Raoulia* was also fairly discernible in the imagery, but often appeared similar, spectrally, to whitish lichen species occurring in association with it; they were therefore grouped into a *Raoulia*-lichen complex.
4. The prostrate native broom species endemic to Kaitorete Spit, *Carmichaelia appressa* (Widodo 1997), most frequently occurred mixed with other herbaceous and grass species. Nonetheless this species had a discernible spectral signature that enabled a prostrate broom complex to be identifiable. Similarly, areas of bryophytes occurring in deflation hollows and back-dune areas in association with exotic herbaceous and grass species could also be relatively well discriminated based on spectral signatures.
5. Both the herbaceous mix and grass mix groups were readily discernible as complexes in most cases. These two groups contained a large number of predominately (but not exclusively) exotic species that have been characterised in other field surveys of Kaitorete Spit (e.g. Peace 1975; Widodo 1997). The mixing between these two groups on the ground, the intermixing of these groups with the other cover types and the effects of management and grazing activities on the vertical structure and spectral reflectance of their constituent species, made it difficult to delineate these cover types accurately in all areas that were examined. The relative abundance of these two cover types may nonetheless provide an overall indication of the areas of the beach that are more 'natural' relative to those that are under pressure from weed invasion, etc.
6. Dead plant material was very challenging to identify visually and spectrally as a cover type.

5.2 Correspondence of image- and field-sampled data

One of the aims of this study was to evaluate the extent to which image-classified cover type information concurred with that derived from rapid, plot-based vegetation surveys. On the whole, UAV-obtained data combined with trained classifications enabled the quantification of the main plant communities occurring across the dune systems in the study area. The identification of individual plants and dominant species was generally consistent with those obtained from field-collected data and results indicated a good correspondence between the relative proportions of the dominant image-based cover types and those quantified in the field. Nonetheless, some cover types were inadequately discriminated in the imagery, which resulted in variability between UAV-based and field-collected cover frequencies. For some cases, such as with prostrate broom, the need to treat it as a component of a mixed cover type meant that its relative abundance was overestimated in comparison with field data. The imagery was also unhelpful for identifying forbs and other small plant species or a variety of exotic grass species; many of these plants were growing as mixtures and there was inadequate spectral separation in comparison with other co-occurring species. Such results emphasise some limitations of using imagery, even at extremely high spatial resolutions, for plant identification. Vegetation is often complex in structure and spectral reflectance qualities, particularly when occurring in mixtures. Using increasingly higher-resolution imagery can only resolve these complexities to a certain point (Peña et al. 2015). The increasing availability of hyperspectral sensors for UAVs may enable further gains in species identification by enabling the spectral un-mixing of plants within pixels using species-specific signatures (Asner et al. 2015). Further, 3D **point clouds** derived from the overlap among UAV-collected images can also provide the means to characterise vegetation structure and topography that can then be used as ancillary data to improve image classifications (Anderson & Gaston 2013).

It is also worth noting that there were other issues that may have caused differences in image-classified v. field-assessed cover types. First, there were accuracy issues in the geo-rectification of the imagery, largely due to inadequate ground control at the time of image collection. This issue, coupled with errors in GPS positioning of field plots, meant that precise imagery overlay with plots was not possible, resulting in misaligned image and ground data at all plot locations. Non-concordance between image classifications and plot cover types may also have occurred as a result of weed re-growth following control activities that had occurred prior to field data collection. One of the most obvious examples of this was the clearly higher amounts of tree lupin in the imagery at plot locations, compared with what was field-sampled in the plots about 10 months prior. When compared with UAV data collected in January 2013, the December 2013 imagery used for our analysis clearly highlighted these temporal changes (Fig. 9). Lupin is a major problem weed on Kaitorete Spit, competing with native plants for resources and causing pulses of nitrogen that encourage the growth of other exotic weeds, especially grasses (Maron & Connors 1996). Lupin is actively controlled by DOC and it is clear that UAV-based imagery can provide an effective means of monitoring the spread of this readily-identifiable species and the efficacy of its management.

6. Conclusions and recommendations

This study showed that an analysis of UAV-collected imagery, using expert knowledge of the vegetation occurring across the dune system at Kaitorete spit, was successful in creating a reasonably accurate cover type classification of this system, and in quantifying the relative abundances of dominant cover types. We suggest that the classification process, and the data generated, can be used as a complement/supplement to field-based surveys, thus potentially reducing overall field costs. Further, UAV-based images collected through time could also provide a useful means to monitor, both visually and quantitatively, changes in the state of the system due to both natural processes and human interventions.

Based on this case study, we recommend:

1. The further exploration of UAV-collected (or other high-resolution) multi-spectral imagery for dune vegetation classification and monitoring to determine how many samples are required for accurate training of the supervised image classifications, and the best way to collect these training samples. In this respect, we recommend that field data should still be collected for training and validation of image analysis.
2. Assessment should also be extended to other ecological systems, to determine best practice in classifying high-resolution, multi-spectral image data collected from UAVs or other aerial platforms for different types of vegetation.
3. That care be taken in the collection and pre-processing of UAV imagery. One ongoing issue is that UAV imagery is easy to collect, even by non-experts. However, to extract accurate and meaningful data from imagery, adequate ground control laid down in the field at the time of flying is required to spatially calibrate imagery to ground locations. This is particularly important when aligning imagery to ground-based survey locations, and in generating accurate 3D point cloud information. Analysts with image processing knowledge are essential for properly deriving orthorectified images that can then be used for analysis.
4. The testing of different supervised image classification methods (e.g. object-oriented classification) and algorithms (e.g. neural networks, regression trees, support vector machines) to determine the most appropriate and accurate solutions for UAV imagery collected in different situations with a variety of vegetation cover types.

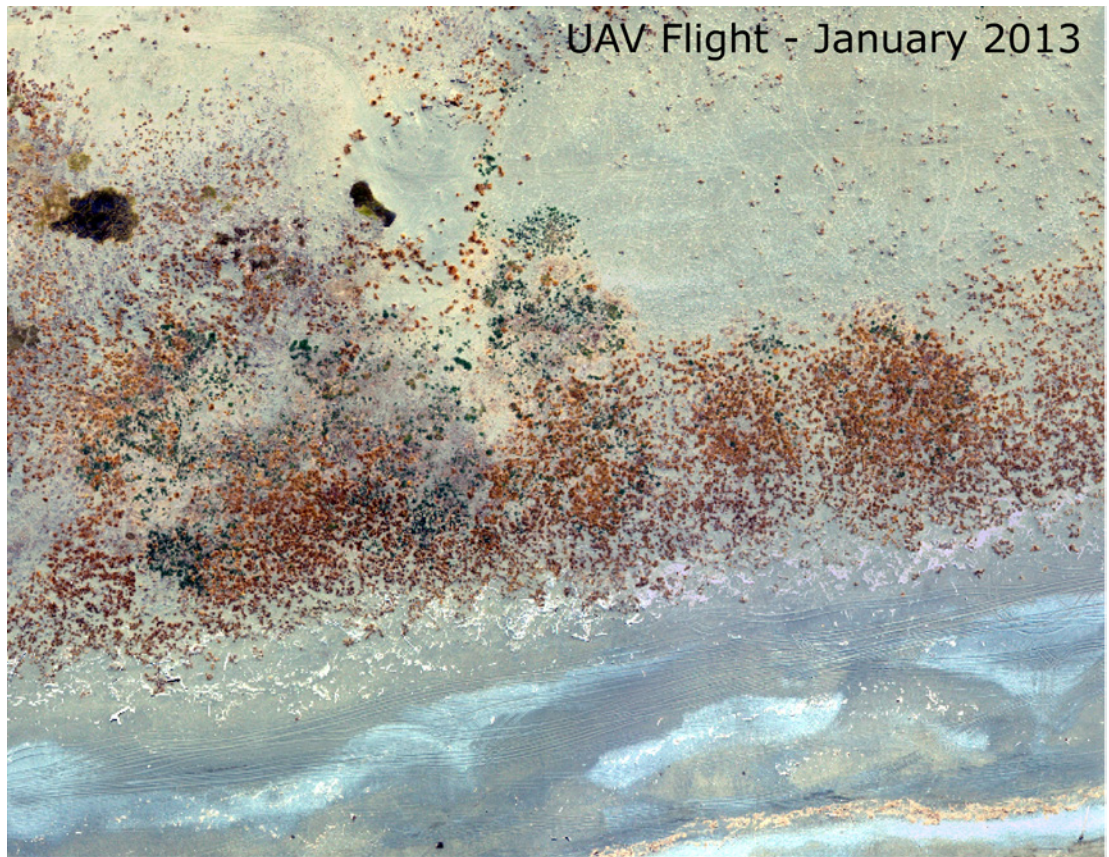


Figure 9. An illustrative example of changes in vegetation between two UAV flights, over a one-year period, at Kaitorete Spit. A population of pīngao (*Ficinia spiralis*) tussocks are visible on the fore dune in the first flight (top image); a year later (bottom image), the readily-visible yellow flowers of tree lupin (*Lupinus arboreus*) indicates the rapidity with which this exotic species has invaded into this zone.

5. Further exploration of the use of UAV-based technologies and data to augment ground surveys. This includes the use of point cloud data to derive high-resolution depictions of terrain and vegetation structure, an exploration of hyperspectral sensors to increase spectral resolution and to help differentiate plant species occurring in mixtures, and the analysis of images through time to evaluate the ability to detect change in cover and to discriminate plant groups based on phenology.
6. That, ultimately, cost-benefit analyses should be carried out to compare the costs of UAV- and field-based monitoring and to determine the value added by having some UAV-based monitoring in addition to field-based monitoring.

7. Acknowledgements

We would like to thank Myles MacIntosh, Anaïs Teiche, Marion Dassonneville, Dirkje Verhoeven for their considerable help with field sampling, and to Aamir Bonamis for his help with components of the image processing and classification. We also thank an anonymous reviewer and the editor for their comments, resulting in a much-improved manuscript.

8. References

- Anderson, K.; Gaston, K.J. 2013: Lightweight unmanned aerial vehicles will revolutionize spatial ecology. *Frontiers in Ecology and the Environment* 11: 138-146.
- Armon, J.W. 1970: Recent shorelines between Banks Peninsula and Cooper's Lagoon. MSc. Thesis, University of Canterbury, Christchurch, New Zealand.
- Asner, G.P.; Martin, R.E.; Anderson, C.B.; Knapp, D.E. 2015: Quantifying forest canopy traits: imaging spectroscopy versus field survey. *Remote Sensing of Environment* 158: 15-27.
- Barringer, J.; McNeill, S.; Pairman, D. 2002: Progress on assessing the accuracy of a high resolution digital elevation model for New Zealand. In: 5th international symposium on spatial accuracy assessment in natural resources and environmental sciences, Melbourne, Australia.
- Breckenridge, R.P.; Dakins, M.; Bunting, S.; Harbour, J.L.; Lee, R.D. 2012: Using unmanned helicopters to assess vegetation cover in sagebrush steppe ecosystems. *Rangeland Ecology & Management* 65: 362-370.
- Callaghan Innovation 2015: So, what is everybody droning on about? <https://www.callaghaninnovation.govt.nz/accelerate-ezine/accelerate-september-2014/so-what-everybody-droning-about>. Retrieved 25 February 2016.
- Cook, D.E.; Strong, P.A.; Garrett, S.A.; Marshall, R.E. 2013: A small unmanned aerial system (UAS) for coastal atmospheric research: preliminary results from New Zealand. *Journal of the Royal Society of New Zealand* 43: 108-115.
- Cruzan, M.B.; Weinstein, B.G.; Grasty, M.R.; Kohm, B.F.; Hendrickson, E.C.; Arredondo, T.M.; Thompson, P.G. 2016: Small unmanned aerial vehicles (micro-UAVs, drones) in plant ecology. *Applications in Plant Sciences* 4: 1600041.
- Department of Lands and Survey 1985: Report on proposed reserve addition to Kaitorete Spit Scientific Reserve. New Zealand Department of Lands and Survey, Christchurch. 34 p.
- DOC (Department of Conservation) & MfE (Ministry for the Environment) 2000: The New Zealand biodiversity strategy. Department of Conservation, Wellington.
- Farmax 2014: Consultant investigates drones to help farmers make better decisions. <http://farmax.co.nz/news-and-resources/media-room/consultant-of-the-year-news/consultant-investigates-drones-to-help-farmers-make-better-decisions/>. Retrieved 25 February 2016.
- Garrett, S.A.; Cook, D.E.; Marshall, R.E. 2011: The Seabreeze 2009 experiment: investigating the impact of ocean and atmospheric processes on radar performance in the Bay of Plenty, New Zealand. *Weather and Climate* 31: 82-100.

- Getzin, S.; Wiegand, K.; Schoning, I. 2012: Assessing biodiversity in forests using very high-resolution images and unmanned aerial vehicles. *Methods in Ecology and Evolution* 3: 397-404.
- Griffiths, J.W.; Paterson, A.M.; & Vink, C.J. 2005: Molecular insights into the biogeography and species status of New Zealand's endemic *Latrodectus* spider species; *L. katipo* and *L. atritus* (Araneae, Theridiidae). *Journal of Archnology* 33: 776-784.
- Hart, J. 2015: Farming for the future – drone technology set to take off. Farmers weekly news. <http://farmersweekly.co.nz/article/farming-for-the-future-drone-technology-set-to-take-off?p=8>. Retrieved 24 February 2016.
- Hilton, M. 2006: The loss of New Zealand's active dunes and the spread of marram grass (*Ammophila arenaria*). *New Zealand Geographer* 62: 105-120.
- Hilton, M.; Duncan, M.; Jul, A. 2005: Processes of *Ammophila arenaria* (marram grass) invasion and indigenous species displacement, Stewart Island, New Zealand. *Journal of Coastal Research* 21: 175-185.
- Hilton, M.; Macauley, U.; Henderson, R. 2000: Inventory of New Zealand's active dunelands. *Science for Conservation* 157. Department of Conservation, Wellington, New Zealand. 35 p.
- Jensen, J.R. 2005: Introductory digital image processing: a remote sensing perspective (3rd edition). Prentice Hall. 526 p.
- Koh, L.P.; Wich S.A. 2012: Dawn of drone ecology: low-cost autonomous aerial vehicles for conservation. *Tropical Conservation Science* 5: 121-132.
- Koski, W.R.; Allen, T.; Ireland, D.; Buck, G.; Smith, P.R.; Macrander, A.M.; Halick, M.A.; Rushing, C.; Sliwa, D.J.; McDonald, T.L. 2009: Evaluation of an unmanned airborne system for monitoring marine mammals. *Aquatic Mammals* 35: 347-357.
- Laliberte, A.S.; Goforth, M.A.; Steele, C.M.; Rango, A. 2011. Multispectral remote sensing from unmanned aircraft: Image processing workflows and applications for rangeland environments. *Remote Sensing* 3: 2529-2551.
- Leathwick, J.; Morgan, F.; Wilson, G.; Rutledge, D.; McLeod, M.; Johnston, K. 2002: Land environments of New Zealand: a technical guide. Ministry for the Environment, Wellington.
- Leathwick, J.R.; West, D.; Gerbeaux, P.; Kelly, D.; Robertson, H.; Brown, D.; Chadderton, W.L.; Ausseil, A.G. 2007: Freshwater ecosystems of New Zealand (FENZ) geodatabase. Version one – August 2010. User guide. Department of Conservation, Wellington.
- Lisein, J.; Michez, A.; Claessens, H.; Lejeune, P. 2015: Discrimination of deciduous tree species from time series of unmanned aerial system imagery. *PLoS ONE*, 10, DOI: 10.1371/journal.pone.0141006
- MacLean, H. 2015: Drone spray helicopter flies by wire. *Otago Daily Times*. <http://www.odt.co.nz/regions/north-otago/360574/drone-spray-helicopter-flies-wire>. Retrieved 24 February 2016.
- Maron, J.L.; Connors, P.G. 1996: A native nitrogen-fixing shrub facilitates weed invasion. *Oecologia* 105: 302-312.
- Nishar, A.; Richards, S.; Breen, D.; Robertson, J.; Breen, B. 2016: Thermal infrared imaging of geothermal environments and by an unmanned aerial vehicle (UAV): a case study of the Wairakei – Tauhara geothermal field, Taupo, New Zealand. *Renewable Energy* 86: 1256-1264.
- Oliphant, J.L. 2014: Pīngao (*Ficinia spiralis*) history and propagation. *Acta horticulturae* 1055: 67-71.
- Patrick, B. 2002: Conservation status of the New Zealand red katipo spider (*Latrodectus katipo* Powell, 1871). *Science for Conservation* 194, Department of Conservation, Wellington, New Zealand. 33 p.
- Peace, M. 1975: The plant ecology of dune system on Kaitorete Spit. MSc. Thesis, University of Canterbury, Christchurch, New Zealand.
- Pegman, A.P.; Rapson, G.L. 2005: Plant succession and dune dynamics on actively prograding dunes, Whatipu Beach, northern New Zealand. *New Zealand Journal of Botany* 43: 223-244.
- Peña, J.M.; Torres-Sánchez, J.; Serrano-Pérez, A.; de Castro, A.I.; López-Granados, F. 2015: Quantifying efficacy and limits of unmanned aerial vehicle (UAV) technology for weed seedling detection as affected by sensor resolution. *Sensors* 15: 5609-5626.
- Quin, M. 2014: Kiwis fly first with drone technology. *NBR*. <http://www.nbr.co.nz/article/kiwis-fly-first-drone-technology-ns-164141>. Retrieved 24 February 2016.
- R Core Team 2017: R: A language and environment for statistical computing. R Foundation for Statistical Computing, Vienna, Austria. URL <https://www.R-project.org/>.
- Ratcliffe, N.; Guihen, D.; Robst, J.; Crofts, S.; Stanworth, A.; Enderlein, P. 2015: A protocol for the aerial survey of penguin colonies using UAVs. *Journal of Unmanned Systems* 3: 95-101.

- Robb, T. 2014: Farm drones: Rise of the machines. *Bay of Plenty Times*. http://www.nzherald.co.nz/bay-of-plenty-times/rural/news/article.cfm?c_id=1503348&objectid=11235843. Retrieved 25 February 2016.
- Sardà-Palomera, F.; Bota, G.; Viñolo, C.; Pallarés, O.; Sazatornil, V.; Brotons, L.; Gomáriz S.; Sardà, F. 2012: Fine-scale bird monitoring from light unmanned aircraft systems. *Ibis* 154: 177–183.
- Taranaki Daily News, 2014: Farmers get low-down on agricultural drones. <http://www.stuff.co.nz/business/farming/agribusiness/10121245/Farmers-get-low-down-on-agricultural-drones>. Retrieved 24 February 2016.
- Tipa, R. 2014: Drone big success on and off farm. *NZ Farmer*. <http://www.stuff.co.nz/business/farming/agribusiness/10471526/Drone-big-success-on-and-off-farm>. Retrieved 25 February 2016.
- Verhoeven, D.; Buckley, H.L.; Curran, T.J.; 2014: Functional traits of common New Zealand foredune species at New Brighton, Canterbury. *New Zealand Journal of Botany* 52: 460–466.
- von Bueren, S.; Burkart, A.; Hueni, A.; Rascher, U.; Tuohy, M.; Yule, I. 2014: Comparative validation of UAV based sensors for the use in vegetation monitoring. *Biogeosciences* 11: 3837–3864.
- von Bueren, S.; Burkart, A.; Hueni, A.; Rascher, U.; Tuohy, M.; Yule, I. 2015: Deploying four optical UAV-based sensors over grassland: challenges and limitations. *Biogeosciences* 12: 163–175.
- Walker, S.; Price, R.; Rutledge, D.; Stephens, T.; Lee, W.G. 2006: Recent loss of indigenous cover in New Zealand. *New Zealand Journal of Ecology* 30: 169–177.
- Widodo, P. 1997: Floristic variation and environmental relationships of sand dune communities at Kaitorete Spit Scientific Reserve. MSc thesis, Lincoln University, Canterbury, New Zealand.
- Wilhelmson, M. 2015: One man and his drone: watch as farmer uses flying robot, fitted with a horn and siren, to herd his flock of 2,000 sheep. *Daily Mail Australia*. <http://www.dailymail.co.uk/news/article-3105294/One-man-drone-Watch-farmer-uses-flying-robot-fitted-horn-siren-herd-flock-2-000-sheep.html>. Retrieved 25 February 2016.
- World Wildlife Fund 2012: New Zealand's environmental record since the original earth summit. WWF, Wellington, New Zealand.
- Wratt, D.S.; Tait, A.; Griffiths, G.; Espie, P.; Jessen, M.; Keys, J.; Ladd, M.; Lew, D.; Lowther, W.; Mitchell, N.; Morton, J.; Reid, S.; Richardson, A.; Sansom, J.; Shankar, U. 2006: Climate for crops: integrating climate data with information about soils and crop requirements to reduce risks in agricultural decision-making. *Meteorological Applications* 315: 305–315.

9. Glossary of terms

Calibration Targets – Targets of known spectral characteristics (usually white and black) that have been placed on the ground before UAV image data collection and are therefore identifiable later in the images. These are used for georeferencing, as well as the calibration of the sensor deployed on the UAV to correct for differences in light conditions and the effect on recorded spectral data.

Geo-referencing – This is achieved using position data collected by a GPS device located on board the UAV, by manually matching features in the image within a GIS software to the same features located on an independent GIS dataset, or by using a combination of these methods.

Ground truth – data collected by direct sampling. In remote sensing, this usually applies to ‘in-situ’ or field-collected data that is used as a reference to infer relationships over the complete area that is being studied. In this study, ground truth measurements refer to the vegetation sample plot data that were collected in the field.

Mosiacing and colour balancing – method of combining adjacent images into a single, seamless image (image mosaic), while balancing differences in spectral data (brightness) at the transitions among adjoining images.

Multispectral imagery – Reflected electromagnetic energy collected by a sensor in both visible and non-visible portions of the spectrum and stored as multiple layers (bands) of data; for example, red, green and blue (RGB) and near-infrared (NIR), together comprising a ‘multispectral image’.

Orthorectification – Method of removing the effects of image perspective (tilt) and terrain (relief) from an image. This technique is usually carried out with specialised software by validating the image against either a known digital elevation model (DEM) or a number of ground control points with known x, y and z coordinates.

Photogrammetric calibration – Photogrammetry is the science of deriving accurate measurements of features (such as the 3-dimensional position on the ground or the top of a building or tree canopy), based on information contained within overlapping portions of adjacent images. To undertake such measurements, photogrammetric calibration is required, whereby geometric coordinates (longitude, latitude and elevation) are used in combination with other variables (such as angle and focal length of a sensor) to accurately assess how each image relates to another and calculate how different pixels have altered geometrically to create the final 3-D model.

Point cloud – a set of points derived from overlapping imagery that define the three-dimensional surface locations of features in the imagery. The 3-D point cloud can be created once photogrammetric calibration of a set of images has occurred.

Spectral data – Different wavelengths (or spectral ‘bands’) of electromagnetic energy reflected from features on the Earth’s surface and recorded in digital form as varying levels of brightness. Spectral data typically comprise reflected energy recorded in the visible (e.g. colour) and non-visible (e.g. infrared) parts of the electromagnetic spectrum.

Stratified random sampling – A sampling technique in which the total sample group is divided into smaller groups or strata. Each group usually has defined characteristics (vegetation cover types in this study). Once these groups have been designated, samples are selected randomly for each group. The total samples for each group can be a defined number or a percentage of the total samples of a given group.

Supervised image classification – The location and class type (cover type in this analysis) of some of the pixels in the image are identified prior to classification. These areas are known as ‘training pixels’ and the spectral characteristics of these training pixels for each class type are

used to subsequently train (or supervise) a classification algorithm to classify the full study site. The best classification results are therefore achieved when there are clear spectral differences (e.g. in red, green, blue, infrared) among the different classes.

Validation pixels – Pixels of known classification type used as a reference in classification accuracy (%) tables. The output classification pixels are overlaid on the validation pixels, and the accuracy of the classification is assessed by determining whether an output classification map pixel of a defined location has the same class as the validation pixel. Validation pixels cannot overlap with any of the ‘training pixels’ used in the classification.